# Performance research of VAWT with expandable blades based on savonius turbines

*Qiuyu* Gu[1], *Zhipeng* Tang[2,*], *Wanna* Chang[2]

[1]Cultural Foundation, Changzhou Vocational Institute of Mechatronic Technology, Changzhou, China
[2]College of Mechanical Engineering, Changzhou Vocational Institute of Mechatronic Technology, Changzhou, China

**Abstract.** In order to improve the wind energy utilization of vertical axis wind turbine (VAWT), this paper presents a new structure of VAWT with expandable blades. The blades of the new turbine are symmetrical airfoil NACA0012 instead of curved blades. The blades of the new structure VAWT have open and folded state. While the blades rotate to the windward side, the blades are open and similar to the curved blades of the S-type turbine. While the blades rotate to the leeward side, the blades are folded and similar to the airfoil of the H-type turbine. In this paper, multi-stream tube theory was used to analyze the movement of the new type VAWT in the flow field, solve the wind speed influencing factors of the model, establish the theoretical formula of wind energy utilization ($C_P$ value) of the new type VAWT. And performance of the wind turbine was simulated and calculated by Matlab. Cp value and self-starting performance of the new type VAWT has greatly improved compared with Savonius type wind turbine. The blade of the new type VAWT is constant section in the vertical direction which can be produced by the costless form of straight blade production. The new type VAWT is not only suitable for medium and large wind farm, but also can be well applied in the areas with relatively poor wind energy resources.

## 1 Introduction

In recent years, environmental pollution and energy exhaustion becoming serious, new energy R&D becomes strategy of national development. Wind energy is one of the rapid development new energy, performance and the $C_P$ value of wind turbine directly affects the use of wind power. Since the blade design, machining and installation of horizontal axis wind turbine is difficult, the blades are sensitivity for wind direction and attack angle, and the start-up wind speed is high, people haven't given up on the R&D in VAWT. But impeller structure results the resistance-type VAWT low $C_P$ value, which limits its development.

Since the impeller structure affects the aerodynamic performance of resistance-type VAWT, the new S-type wind turbine structure began to become the focus of the research,

* Corresponding author: tzp2192@czimt.edu.cn

some new structure achieved relatively good results such as: overlap ratio of blades[1], cross section of blades[2], twist blade[3], the number of layers and blades[4], layout angle of blade[5], semi-automatic valve structure[6], lift-drag complementary blades and other new structures[7,8].

In theoretical research, since the flow field of S-type turbine is complex, the theoretical research immature which restricted its development. For the current theoretical research methods for flow field analysis of S-type turbine are as follows: flow tube method, vortex method and CFD methods based on fluid theory. These methods have good effect on the performance research of turbine, shorten research cycle and so on.

A new VAWT with expandable blades was researched in this paper. The airfoil blades of the turbine have open and folded states. During operation, the blades will open in the windward side, which improves the driving torque of the turbine. And the blades will fold in the leeward side, which reduces the drag torque of the turbine. Meanwhile, the cross section of the folded blades are sections, the blades can also have some driving torque in appropriate angle when subject to leeward flow. Therefore, the new VAWT can increase rotational torque in three ways, which greatly improves the $C_P$ value. In addition, when the turbine starts up, under the condition that the inside of open blade is on the flow direction and the chord of folded blade is parallel to the flow direction, the windward area of the blades remain constant and the leeward area reduce which increases the starting torque compared to S-type turbine. This paper uses flow tube method to simulate performance of the new VAWT with expandable blades. By computing the $C_P$ value of turbine with different structure parameters to obtain the maximum $C_P$ value of this kind of new VAWT.

## 2 Physical model

Since the blades have open and folded states, the airfoil blade can be divided into two parts, each of which can rotate around the airfoil vertex with certain angle. Windward side of the symmetrical open blade is similar to curved blade of S-type turbine blade, and the folded state blade is similar to airfoil blade of the H-type turbine. According to thickness, quality, and starting performance, this paper selects NACA0012 symmetric airfoil, shown in Figure 1.

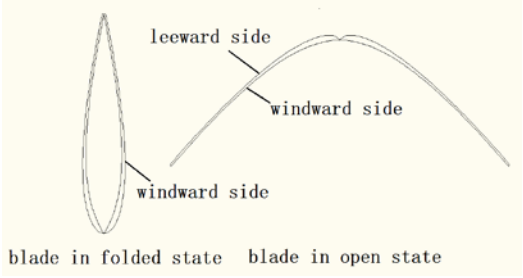


**Fig. 1.** The structure of the blades in new type wind turbine**.**

Figure 2 is the operation of the new VAWT blades in every 10° of a working cycle.

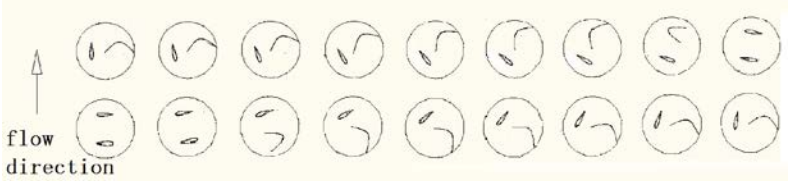


**Fig. 2.** The operation of the blades in new type wind turbine.

Since the expandable blade is straight blade, Fig.3a) shows the position of the blade when time=0 and time=t (the self-rotation center coordinate position of is $O_1(x, y)$: $x=OO_1\sin\varphi$, $y=OO_1\cos\varphi$, $\varphi=\omega_t$) in any two-dimensional horizontal section.

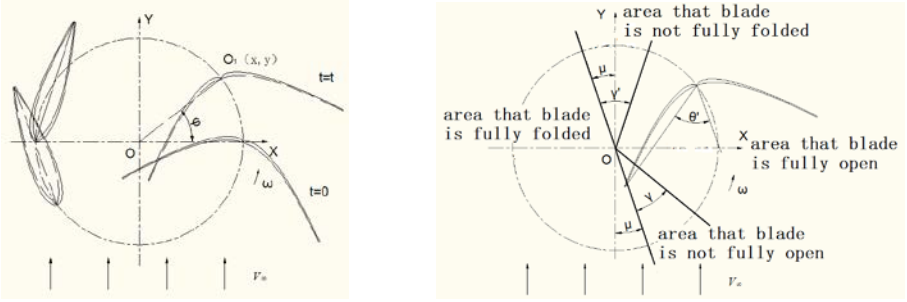


a) The position of the blade when t=0 and t=t b) The division of the calculating region

**Fig. 3.** The position of the blade of the blade motion analysis.

The rotation cycle is divided into four calculation regions based on the state of the blade: the area that the blade is not fully open, fully open, not completely folded, fully folded, shown in Fig.3b) θ' is the maximum unilateral open angle of the blade, γ is the revolution angle of the rotor corresponding to the self-rotation open angle of the blade, γ' is the revolution angle of the rotor corresponding to the self-rotation folded angle of the blade and μ is the angle that the blade symmetry axis relative to the starting position angle when the symmetry axis of the blade is parallel Y-axis. The formula can be obtained when the blade rotate constantly:

$$\frac{\gamma'}{\omega}=\frac{\theta'\pm\gamma'}{\omega_C} \tag{1}$$

$$\frac{\gamma}{\omega}=\frac{\theta'\mp\gamma}{\omega_O} \tag{2}$$

where in $\omega_C$——Self-rotating angular velocity when the blades fold(rad/s);

$\omega_O$——Self-rotating angular velocity when the blades open(rad/s);

The "+" sign in formula (1) means the blade near position "O" in Fig.4, and the "-" sign means the blade away from "O". The symbols result in formula (2) just opposite.

From the above analysis it shows that main factors affecting performance of new VAWT with expendable blade are as follows:

(1) θ': θ' should ensure the inside of the windward side an arc with smooth curvature. Oversized θ' makes the blade flat-panel, too small θ' greatly reduces the swept area of turbine.

(2) γ: γ should minimize the impact of open movement on the overall operation of the blade, small γ makes the blade drive the turbine in windward area as soon as possible. but too small γ makes the open process consumes less time, which has great impact on the turbine.

(3) γ': γ' should make the blade maintain open with large angel in effective work area to improve CP value. Considering the latter half of the folding process, the central portion of the blade is driven by the wind. The blade will suffer great resistance if the opening angle is too large. But too small γ' will cost the folding process less time, which has impact on the turbine.

# 3 Stress analysis

## 3.1 Stress analysis of the blade in the area without fully open

The blade is S-shaped curved blade in the open state, the force driven by the wind is related to the blade chord projected area that in the direction perpendicular to the wind flow. The $B_{12}$ blade is driven by wind to open, it did not produce a driving torque to "O". The $B_{11}$ blade is open against the wind, its energy consumption comes from inside of turbine system. The range of the angle is $3\pi/2+\mu<\varphi<3\pi/2+\mu+\gamma$, as shown in Fig.4a).

According to formula (2), the projected area of $B_{11}$ blades perpendicular to wind flow is:

$$S_1 = l_{O_1L}\cos\angle LO_1E = l_{O_1L}\cos\left[\frac{\theta'+\gamma}{\gamma}\left(\varphi-\frac{3\pi}{2}-\mu\right)\right] \tag{3}$$

The force F1 on the blade driven by wind flow is as follows:

$$F_1 = \frac{1}{2}\rho S_1 \cdot {V_{Ry}}^2 C_d \tag{4}$$

where in ρ——density of air,
$C_d$——drag coefficient of the blade
$V_{Ry}$——relative inflow speed near the blade ($V_R$) projection on the flow direction.
Tip speed ratio (TSR):

$$\lambda = U_b / V_\infty \tag{5}$$

wherein $V_\infty$ ——wind velocity from infinity,

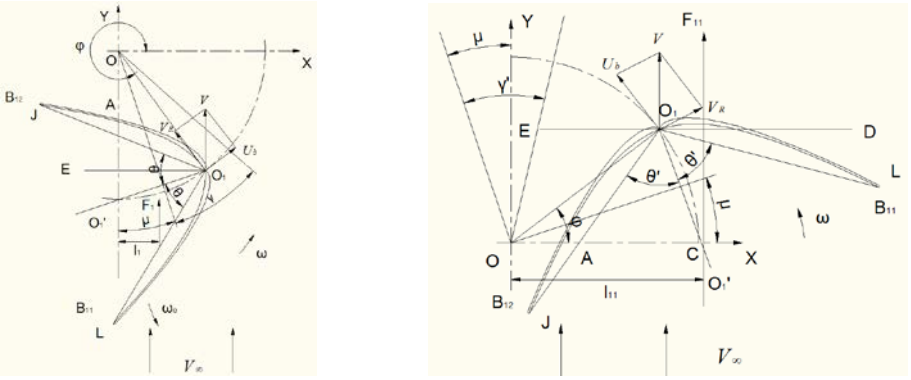


a) The force analysis while blades with overlap b) The force analysis while blades without overlap

**Fig. 4.** The force analysis while the blades are opening.

Since $V_\infty$ is disturbed by the rotating blades, the wind speed decreased to V when it reaches to the blade. The speed-inducible factor "a" is used to describe V accurately.

$$a = (V_\infty - V)/V_\infty \tag{6}$$

$$V_{Ry} = V_\infty\left(1-a-\lambda\cos\varphi\right) \tag{7}$$

The arm of torque from F1 to the turbine center $l_1$, and torque $M_1$ are as follows:

$$l_1 = \left| l_{OO_1} \cos(2\pi - \varphi) - \frac{1}{2} S_1 \right| = \left| l_{OO_1} \cos\varphi - \frac{1}{2} l_{O_1L} \cos\left[ \frac{\theta' + \gamma}{\gamma} \left( \varphi - \frac{3\pi}{2} - \mu \right) \right] \right| \tag{8}$$

$$M_1 = F_1 \cdot l_1 \tag{9}$$

### 3.2 Stress analysis of the blade in the area with fully open

(1) The projection of the blade $B_{12}$ and $B_{11}$ is not overlapped. And the rotating angle is $2\pi - \theta' + \mu < \varphi < 2\pi$ or $0 < \varphi < \mu + \theta'$, shown in Fig.4b).

The force $F_{11}$ on the blade driven by wind flow is as follows:

$$\begin{aligned} F_{11} &= \frac{1}{2} \rho S_{11} \cdot V_{Ry}{}^2 C_d \\ &= \frac{1}{2} \rho l_{O_1J} \left[ \sin(-\varphi + \theta' + \mu) + \sin\left(\varphi + \theta' - \mu\right) \right] V_\infty{}^2 \left(1 - a - \lambda \cos\varphi\right)^2 C_d \end{aligned} \tag{10}$$

$$\begin{aligned} l_{11} &= l_{OO_1} \cos\varphi + \frac{S_{11}}{2} - l_{O_1J} \cos(\frac{\pi}{2} + \varphi - \theta' - \mu) \\ &= l_{OO_1} \cos\varphi + \frac{1}{2} l_{O_1J} \left[ \sin\left(\varphi + \theta' - \mu\right) - \sin(-\varphi + \theta' + \mu) \right] \end{aligned} \tag{11}$$

The torque generated by the blade is:

$$M_{11} = F_{11} \cdot l_{11} \tag{12}$$

(2) There are two situation when the projection of the blade $B_{12}$ and $B_{11}$ is overlapped.

One of the situation is the blade $B_{11}$ has blocking effect on $B_{12}$. And the rotating angle is $3\pi/2 + \mu + \gamma < \varphi < 2\pi - \theta' + \mu$, shown in Fig.5a).

The force $F_{12}$ on the blade driven by wind flow is as follows:

$$F_{12} = \frac{1}{2} \rho l_{O_1J} \sin\left(-\varphi + \theta' + \mu\right) \cdot V_\infty{}^2 \left(1 - a - \lambda \cos\varphi\right)^2 C_d \tag{13}$$

The arm of torque from $F_{12}$ to the turbine center $l_{12}$, and torque $M_{12}$ are as follows:

$$l_{12} = l_{OO_1} \cos\varphi - \frac{1}{2} l_{O_1J} \sin\left(-\varphi + \theta' + \mu\right) \tag{14}$$

$$M_{12} = F_{12} \cdot l_{12} \tag{15}$$

The other situation is the blade $B_{12}$ has blocking effect on $B_{11}$, And the rotating angle is $\mu + \theta' < \varphi < \pi/2 + \mu - \gamma'$, shown in Fig.5b).

The force $F_{22}$ on the blade, arm of torque $l_{22}$, and torque $M_{22}$ are as follows:

$$F_{22} = \frac{1}{2} \rho l_{O_1L} \sin\left(\varphi + \theta' - \mu\right) V_\infty{}^2 \left(1 - a - \lambda \cos\varphi\right)^2 C_d \tag{16}$$

$$l_{22} = l_{OO_1} \cos\varphi + \frac{1}{2} l_{O_1L} \sin\left(\varphi + \theta' - \mu\right) \tag{17}$$

$$M_{22} = F_{22} \cdot l_{22} \tag{18}$$

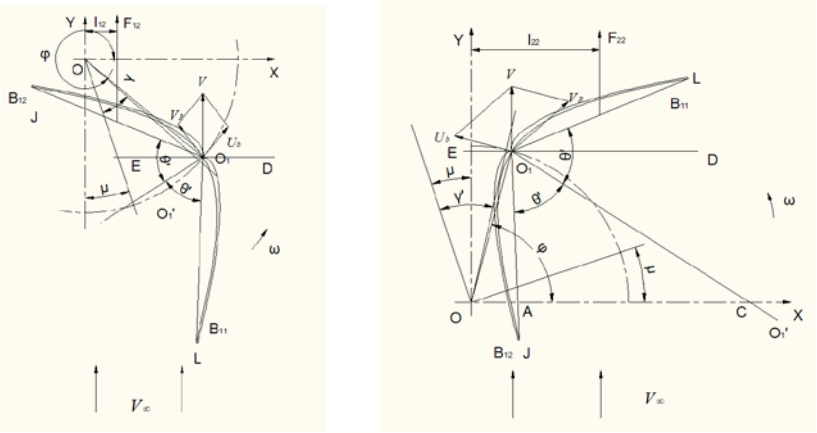

a) $B_{11}$ blade has barrier over $B_{12}$ blade. b) $B_{12}$ blade has barrier over $B_{11}$ blade.

**Fig. 5.** The force analysis while overlap exists in the projection of $B_{11}$ and $B_{12}$ blade.

### 3.3 Stress analysis of the blade in the area without fully folded

When the blade blade is not fully folded, the $B_{12}$ blade did not produce a driving torque to "O". The $B_{11}$ blade is open against the wind, its energy consumption comes from inside of turbine system. The range of the angle is $\pi/2+\mu-\gamma' < \varphi < \pi/2+\mu$, as shown in Fig.6a).

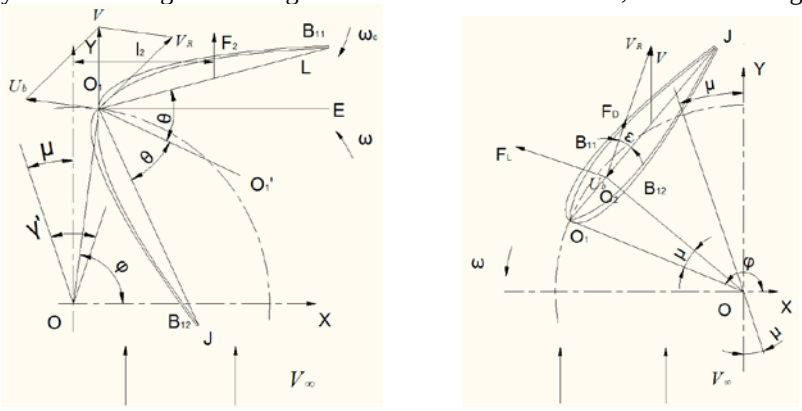

a) The force analysis while the blades are folding b) The force analysis while the blades are fold

**Fig. 6.** The force analysis while the blades are in the folding area.

The force $F_2$ on the blade, arm of torque $l_2$, and torque $M_2$ are as follows:

$$F_2 = \frac{1}{2}\rho l_{O_1L} \cos\left[\frac{\theta'-\gamma'}{\gamma'}\left(\varphi-\frac{\pi}{2}-\mu+\gamma'\right)\right]\cdot V_\infty^{\,2}\left(1-a-\lambda\cos\varphi\right)^2 C_d \tag{19}$$

$$l_2 = l_{OO_1}\cos\varphi + \frac{1}{2}S_2 = l_{OO_1}\cos\varphi + \frac{1}{2}l_{O_1L}\cos\left[\frac{\theta'-\gamma'}{\gamma'}\left(\varphi-\frac{\pi}{2}-\mu+\gamma'\right)\right] \tag{20}$$

$$M_2 = F_2 \cdot l_2 \tag{21}$$

### 3.4 Stress analysis of the blade in the area with fully folded

The range of the angle is $\pi/2+\mu<\varphi<3\pi/2+\mu$, the center of the force in the blade is $O_2$ which is 1/4 length of the blade of the chord, as shown in Figure 6b).

The attack angle of the blade ε and the velocity of the blade $V_R$:

$$\varepsilon = \arctan\frac{V_{Rn}}{V_{R\tau}} \tag{22}$$

$$\left|V_R\right| = \sqrt{{V_{Rn}}^2 + {V_{R\tau}}^2} = \left|V_\infty\right|\sqrt{(1-a)^2+\lambda^2-2(1-a)\lambda\cos(\pi-\varphi+\mu)} \tag{23}$$

Driving torque generated by Fτ (tangential component of lift force $F_L$ and drag force $F_D$):

$$\begin{aligned} M_3 &= F_\tau \cdot l_{OO_2} = (F_L\sin\varepsilon - F_D\cos\varepsilon)\cdot l_{OO_2} \\ &= (\frac{1}{2}\rho l_{O_1J}\cdot\left|V_R\right|^2\cdot C_l\cdot\sin\varepsilon - \frac{1}{2}\rho l_{O_1J}\cdot\left|V_R\right|^2\cdot C_d\cdot\cos\varepsilon)\cdot l_{OO_2} \end{aligned} \tag{24}$$

To sum up: the average torque M and power $P_C$ in rotary of one week by the blade is:

$$M = \frac{2H}{2\pi}\int(-M_1+M_{11}+M_{12}+M_{22}-M_2+M_3)d\varphi \tag{25}$$

$$P_C = M\cdot\omega \tag{26}$$

wherein H——the height of the blade (m).

And the wind energy utilization of turbine ($C_P$) is as follows: $C_P = P_C/(0.5\cdot\rho\cdot A\cdot V^3)$.

## 4 Results and discussion

The parameter “a” from different region of the upstream tube can be obtained by double-multiple stream tube theory when the parameters of the blade and the TSR are different. Under the conditions that θ', γ, γ'and λ are different, the downstream flow tube is divided into the corresponding interval to solve “a”, $C_P$ and other parameters in each interval.

In the new VAWT studied in this paper, the airfoil blade revolution radius is 560mm, blade thickness is 8mm, blade height is 1000mm. Taking the selection condition of structural parameter into account, this paper select θ' as 45°, 50°, 55°, 60°, 65° and 70°, γ as 10°, 15°, 20° and 25°, γ' as 15°, 20°, 25°, 30°, 35°, 40° and 45°. These parameters as used as variables in the calculaton of the new VAWT model. The calculation results and $C_P$-λ curve are obtained in Fig.10 to Fig.15.

### 4.1 Regular pattern of θ' impact on wind turbine performance

Fig.7 is the $C_P$-λ curve of the new VAWT on conditon that γ'=15°. It shows that when γ and γ' is constant, the trend of maximum $C_P$ in each figures is increasing at first and then decreasing along with the increasing of θ'. $C_P$ is the maximum value when θ' is 55°. When γ' and θ' is constant, the trend of maximum $C_P$ in each figures is increasing along with the increasing of γ. $C_P$ is the maximum value when γ is 25°.

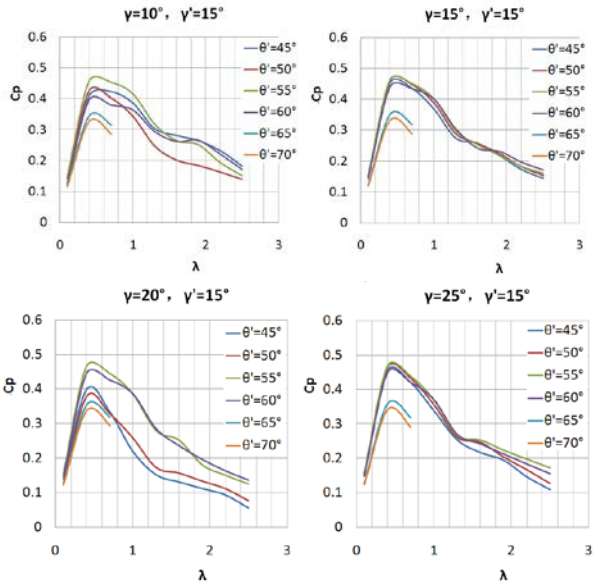


**Fig. 7.** The $C_P$—λ curve of the new turbine while γ'=15°.

Fig.8 is the $C_P$-λ curve of new VAWT on condition that γ=20°. from Fig.7 while γ=25° and Fig.8 we can know that when γ and γ' are constant, the trend of maximum $C_P$ is increasing at first and then decreasing along with the increasing of θ', expect γ'=40°. $C_P$ gets the maximum value when θ' is 55°, expect γ'=40° and γ'=45°. While γ' is 40°, the maximum $C_P$ values is obtained corresponding to θ'=40°. While γ' is 45°, the maximum $C_P$ value is obtained corresponding to θ'=60°. When γ is constant, the trend of maximum $C_P$ in each figures is increasing along with the increasing of γ'. And γ' is 25° when the curve get the peak.

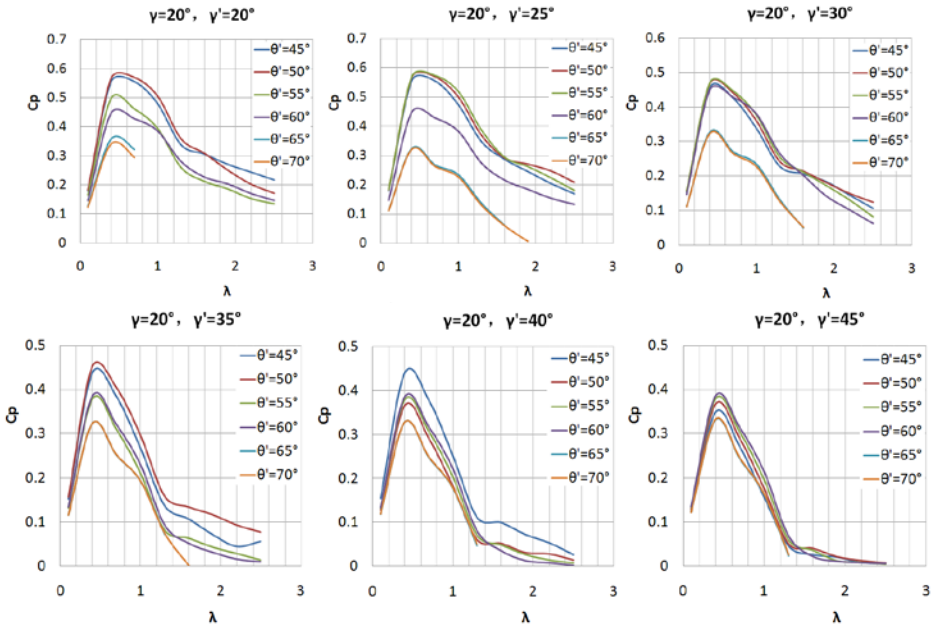


**Fig. 8.** The $C_P$-λ curve of the new turbine while γ=20°.

From the analysis above, it shows that most of the new VAWT obtain the optimum utilization of wind energy while θ' is 55°. The inside of the blade section should be smooth change of curvature when the blade is fully open. So that too large θ' will make the curvature change rapidly, even the section will be "M" shape. It brings unnecessary turbulence when the flow is discharged from the blade in windward area which not only consume wind energy, but also interferes with the flow pushing blade. In addition, the resistance increases when the blade is opening and folding with the increasing of θ'. All of these will weaken the performance of the turbine.

### 4.2 Regular pattern of γ impact on wind turbine performance

Fig.9 is the $C_P$-λ curve of the new VAWT on conditon that γ'=25°. It shows that when θ' and γ' are constant, the trend of maximum value of $C_P$ in each curve at first increase then decrease with the increasing of γ. $C_P$ gets the maximum value when γ' is 55°, expect θ'=65° and θ'=70°. While θ'=65° and θ'=70°, the maximum $C_P$ values is obtained corresponding to γ=20°. When γ' is constant, with θ' increases, the trend of maximum value in the $C_P$-λ curve is at first increase then decrease. And θ' is 55° when the curve get the peak.

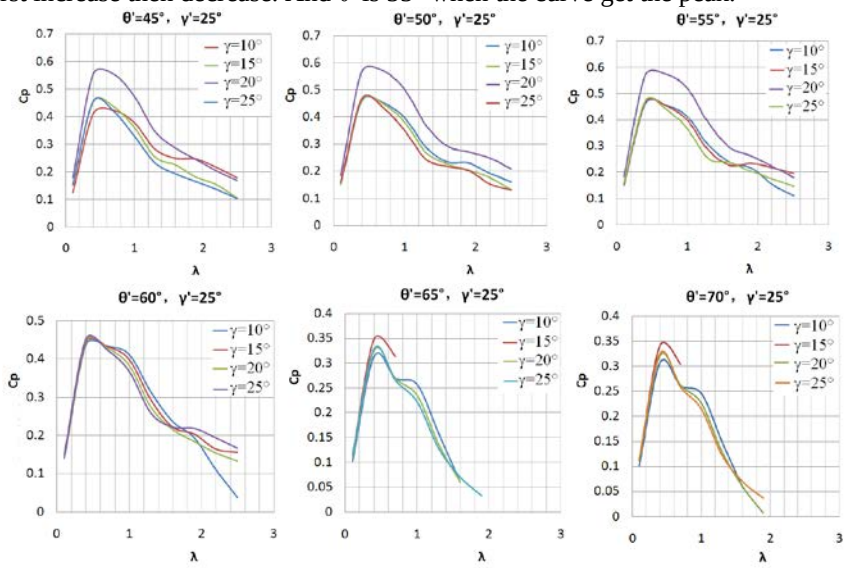


**Fig. 9.** The $C_P$-λ curve of the new turbine while γ'=25°.

Fig.10 is the $C_P$-λ curve of the new VAWT on conditon that θ'=25°. It shows that when γ and γ' are constant, the trend of maximum value of $C_P$ in each curve at first increase then decrease with the increasing of θ'. $C_P$ gets the maximum value when γ is 20°, expect γ'=40° and γ'=45°. While γ'=40° and γ'=45°, the maximum $C_P$ values is obtained corresponding to γ=20°. When θ' is constant, with γ' increases, the trend of maximum value in the $C_P$-λ curve is at first increase then decrease. And γ' is 25° when the curve get the peak. This is consistent with the results of Fig. 8.

From the analysis above, it shows that most of the new VAWT obtain the optimum utilization of wind energy while γ is 15° or 20°. In the actual self-rotation process, the opening time of the blade decrease if γ is too small. The output parameters such as force and acceleration of the opening mechanism will increase sharply which has great impact on the wind turbine. In order to make more use of airflow energy and the blades enter the state of output driving torque as soon as possible in windward area, γ can not be selected too large.

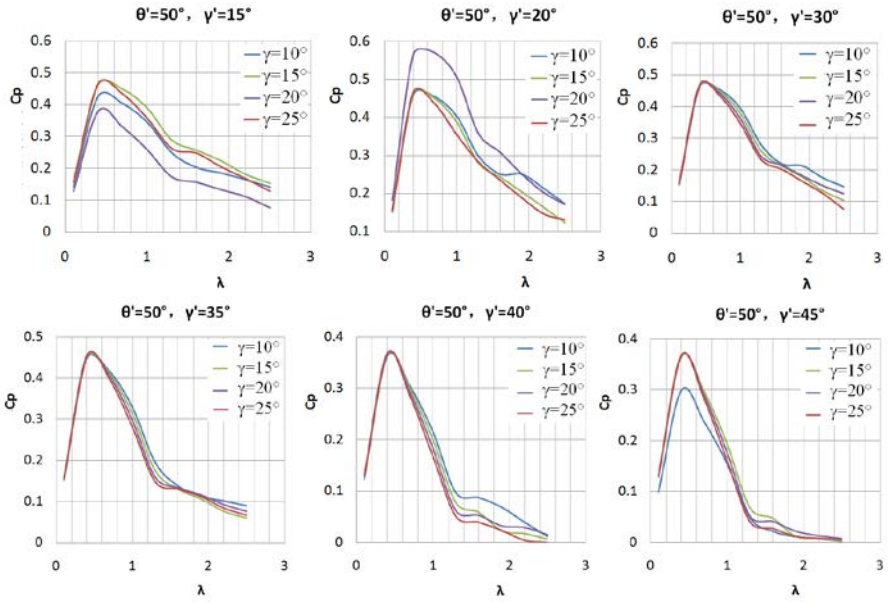


**Fig. 10.** The $C_P$-λ curve of the new turbine while θ'=50°.

### 4.3 Regular pattern of γ' impact on wind turbine performance

Fig.11 is the $C_P$-λ curve of the new VAWT on conditon that θ'=55°. It shows that when γ=20°, θ' and γ are constant, the trend of maximum value of $C_P$ in the curve at first increase then decrease with the increasing of γ'. $C_P$ gets the maximum value when γ' is 25°. The trend of maximum value of $C_P$ in the other curves increase with the increasing of γ'. $C_P$ gets the maximum value when γ' is 15°. When θ' is constant, with γ increases, the trend of maximum value of the curve is at first increase then decrease. And γ is 20° when the curve get the peak.

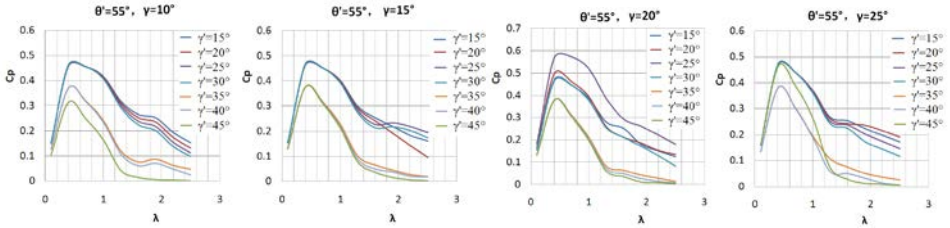


**Fig. 11.** The $C_P$—λ curve of the new turbine while θ'=55°.

Fig.12 is the $C_P$-λ curve of the new VAWT on conditon that γ=10°. It shows that when γ is constant and θ'=45° and θ'=55°, the trend of maximum value of $C_P$ in the curves decrease with the increasing of γ'. $C_P$ gets the maximum value when γ' is 15°. The trend of maximum value of $C_P$ in the other curves at first increase then decrease with the increasing of γ'. $C_P$ gets the maximum value when γ' is 20°. When γ is constant, with θ' increases, the trend of maximum value in the $C_P$-λ curve is at first increase then decrease. And θ' is 55° when the curve get the peak. This is consistent with the results of Fig.9.

From the analysis above, it shows that most of the new VAWT obtain the optimum utilization of wind energy while γ' is 15° or 20°. In the actual process, the suitable γ' can

reduce wind resistance in the folding process and reduce the impact on the turbine. All of these can reduce the wind energy consumption and improve the performance of the turbine.

From the analysis above, it shows that when the θ' is 55°, γ is 20° and γ' is 25°, the new VAWT can get the maximum utilization of wind energy, the maximum of $C_P$ is 0.5738 and the corresponding TSR is 0.7. The range of effective TSR is from 0.3 to 1.15. The maximum $C_P$ value of conventional S-type turbine is 0.2, the corresponding TSR is 0.63, and the range of effective TSR is from 0.35 to 0.95[9]. It shows that the maximum $C_P$ and optimum TSR of the new VAWT has greatly improved compared with the S-type turbine. The range of wind speed application has greatly improved compared with the S-type turbine. The new VAWT can obtain the maximum wind energy in area with great difference of wind speed. Therefore, on the condition of reasonable structural parameters, the performance of the new VAWT with expandable blades is much better than the S-type turbine.

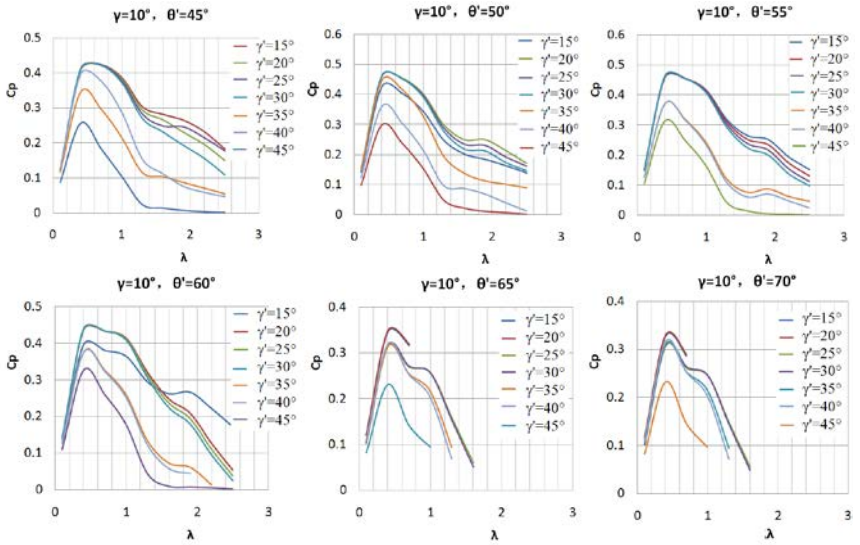


**Fig. 12.** The $C_P$-λ curve of the new turbine while γ=10°.

## 5 Conclusions

In this paper, a new structure VAWT with expandable blade is put forward which is based on reducing wind resistance when the blades are in the leeward area. The principle of generating torque is similar with the S-type turbine when the blade is open to push the turbine in the windward area. The blade is folded in the leeward area, and the section is similar with the H-type turbine. The resistance of the wind can be reduced in leeward area.

Stress analysis and calculation methods are proposed to analyze the motion and force of the new VAWT. In this paper, the calculation area near the turbine flow field is divided and the speed-inducible factor is calculated in each new area by using multi-stream tube theory. Finally, the utilization of wind energy of the new VAWT under the conditions of different parameters such as the max unilateral open angle of the blade (θ'), the revolution angle of the rotor corresponding to the self-rotation open angle of the blade (γ), the revolution angle of the rotor corresponding to the self-rotation folded angle of the blade (γ') and the tip speed ratio (TSR) is solved to determine the optimum blade structural parameters. According to the final results, the maximum $C_P$ value is 57.38% on condition that γ=20°, γ'=25° and θ'=55°. The optimum TSR is 0.7, and the range of effective TSR is from 0.3 to 1.15.

## References

1. Sukanta Roya， Ujjwal K. Saha. Computational study to assess the influence of overlap ratio on static torque characteristics of a vertical axis wind turbine[J]. Procedia Engineering. 2013, 51：694-702.
2. A Kianifar, M Anbarsooz. Blade curve influences on the performance of Savonius rotors: experimental and numerical[J]. Power and Energy. 2011, 225：343-350
3. M.A. Kamoji, S.B. Kedare, S.V. Prabhu. Performance tests on helical Savonius rotors[J]. Renewable Energy. 2009, 34:521-529
4. Saha UK, Thotla S, Maity D. Optimum design configuration of Savonius rotor through wind tunnel experiments[J]. Journal of Wind Engineering and Industrial Aerodynamics. 2008, 96: 1359–75
5. M. A. Kamoji, S. B. Kedare and S. V. Prabhu. Experimental investigations on single stage, two stage and three stage conventional Savonius rotor. International Journal of Energy Research. 2008, 32:877 – 895
6. Thotla, S. Optimum design configuration of Savonius rotor through wind tunnel testing. Guwahati, India:Department of Mechanical Engineering, IIT. M.Tech. Thesis, 2006:3-28.
7. R. Gupta, A. Biswas, K.K. Sharma. Comparative study of a three-bucket Savonius rotor with a combined three-bucket Savonius – three-bladed Darrieus rotor. Renewable Energy. 2008, 33:1974 – 1981
8. K. Pope , V. Rodrigues , R. Doylea, A. Tsopelas , R. Gravelsins , G.F. Naterer , E. Tsang. Effects of stator vanes on power coefficients of a zephyr vertical axis wind turbine[J]. Renewable Energy. 2010, 35:1043–1051
9. Y.X. Yao, Z.P. Tang, X.W. Wang. Optimal design of a drag driven VAWT with a tower cowling. Journal of Wind Engineering & Industrial Aerodynamics. 116 (2013) 32 – 39